

Phosphine oxide-functionalized polyfluorene derivatives: Synthesis, photophysics, electrochemical properties, and electroluminescence performance

GUO ZengShan¹, LIU DeAng³, WANG Cheng¹, PEI Jian^{1*}, ZHOU ZhangLin^{2*}, ZHAO LiHua², GIBSON Gary², BRUG James², LAM Sity² & MAO Samuel S.^{3*}

¹Key Laboratory of Bioorganic Chemistry and Molecular Engineering of Ministry of Education; College of Chemistry and Molecular Engineering, Peking University, Beijing 100871, China

²Information Surfaces Lab, Hewlett Packard Labs, Hewlett Packard Company, 1501 Page Mill Road, Palo Alto, CA 94304, USA

³Lawrence Berkeley National Laboratory and Department of Mechanical Engineering, University of California, Berkeley, CA, USA

Received December 15, 2010; accepted January 8, 2011

A series of phosphine oxide-functionalized polyfluorene derivatives, PFH-PO-40-1 (**P1**), PFH-PO-20-1 (**P2**), PFH-PO-10-1 (**P3**), and PFH-PO-1-1 (**P4**), were prepared via a palladium-mediated Suzuki cross-coupling reaction. The structures and purities of all polymers were fully characterized by ¹H and ¹³C NMR, UV-vis and photoluminescent spectroscopy, gel permeation chromatography, and TGA/DSC. Their emission features showed single broad peaks at about 445 nm in film, compared with those in dilute solutions, which might be caused by some degree of aggregation in the excited states of the backbones. The best electroluminescence (EL) performance of these polymers with configuration of ITO/PEDOT:PSS/Polymer/Alq₃/LiF/Al was obtained from **P1** (current efficiency was 4.2 Cd/A at 6V).

organic light-emitting diodes, polyfluorene derivatives, electroluminescence

1 Introduction

π -Conjugated polymers with electronically rigid backbones have attracted considerable interest due to their electronic and optoelectronic applications, such as organic light-emitting diodes (OLEDs) [1], organic field effect transistors (OFETs) [2], and photovoltaics [3], as well as other organic semi-conducting devices. Polyfluorene derivatives (PFs) have emerged as a class of promising optoelectronic materials, due to their strong blue electroluminescence (EL), high thermal/chemical stability, good solubility in common organic solvents, and facile modification of the side chains without affecting the conjugation of the main chain [4]. Up to now, PFs with a variety of functional groups in the side

chains such as ionic groups or special receptors have been used in several fields such as chemo/biosensors [5] and PLEDs [6].

Phosphine oxide groups have been widely used in the preparation of quantum dots due to their strong affinity for inorganic nanocrystals [7]. In addition, phosphine oxide groups were embedded into conjugated polymers to form hybrid nanocomposites between polymers and nanocrystal and realize efficient Förster energy transfer from the polymer to nanocrystal [8]. Wang's group previously reported PFs with phosphonate/phosphonic acid groups in the side chains which both showed high sensitivity and selectivity towards Fe³⁺ ion [5]. Herein, we design and synthesize a series of PFs via the introduction of phosphine groups into PFs in order to endow these polymers multifunctional properties, especially in electroluminescence. Our PF derivatives reported herein possesses good thermal stability, large band

*Corresponding author (email: jianpei@pku.edu.cn; zhang-lin.zhou@hp.com; ssmao@newton.berkeley.edu)

gap, and good film-forming properties. The electroluminescence (EL) properties of these polymers are recorded on an organic light-emitting diode (OLED) device configuration of ITO/PEDOT:PSS/Polymer/Alq₃/LiF/Al. The best device result (Current efficiency was 4.2 Cd/A at 6V) is obtained from polymer **P1**, which might be due to that the hole and electron in this device had the smallest energy barrier.

2 Experimental

2.1 General experimental

Chemicals were purchased and used as received. All air and water sensitive reactions were performed under nitrogen atmosphere. Toluene and THF were distilled from sodium. ¹H and ¹³C NMR spectra were recorded on a Varian Mercury 300 MHz or Mercury plus 400 MHz using CDCl₃ as solvent unless otherwise noted. All chemical shifts were reported in parts per million (ppm). ¹H NMR chemical shifts were referenced to TMS (0 ppm) or CHCl₃ (7.26 ppm), and ¹³C NMR chemical shifts were referenced to CDCl₃ (77.23 ppm). Absorption spectra were recorded on PerkinElmer Lambda 35 UV-vis Spectrometer. PL spectra were carried out on a PerkinElmer LS55 Luminescence Spectrometer. MALDI-TOF mass spectra were recorded on a Bruker BIFLEX III or AUTOFLEX III time-of-flight (TOF) mass spectrometer (Bruker Daltonics, Billerica, MA, USA) using a 337 nm nitrogen laser with dithranol as the matrix. Elemental analyses were performed using a German Vario EL III elemental analyzer. Differential scanning calorimetry analyses were performed on a METTLER TOLEDO Instrument DSC822° calorimeter. GPC was obtained through a Waters GPC 2410 with a refractive index detector in THF using a calibration curve of polystyrene standards. Thermal gravimetric analyses (TGA) were measured on Thermal Analysis SDT2960. Cyclic voltammetry was performed using BASI Epsilon workstation and measurements were carried out in acetonitrile containing 0.1 M *n*Bu₄NPF₆ as a supporting electrolyte. The carbon electrode was used as a working electrode and a platinum wire as a counter electrode, all potentials were recorded versus Ag/AgCl (saturated) as a reference electrode. The scan rate was 100 mV s⁻¹. EL spectrum was recorded on a Hitachi F-7000 fluorescence spectrophotometer.

2.2 Synthesis

Diocetylphosphine oxide (2)

To a solution of *n*-C₈H₁₇MgBr in Et₂O (2.0 M, 30 mL) was added a solution of di-*n*-butylphosphite (3.92 mL, 20 mmol) in THF (50 mL) under N₂ at room temperature. The mixture was refluxed for 4 h. H₂SO₄ aqueous solution (25%, 40 mL) was added during the period of 30 min at room temperature. The mixture was then extracted with EtOAc three times.

The organic layers were combined, washed with brine, and then dried over Na₂SO₄. After removal of the solvents under reduced pressure, the residue was purified by recrystallization in hexane to give **2** as a white solid (3.8 g, 69%). ¹H NMR (300 MHz, CDCl₃, ppm): δ = 1.88–1.96 (m, 4H), 1.58–1.84 (m, 8H), 1.28–1.42 (m, 20H), 0.86–0.90 (t, *J* = 6.6 Hz, 6H). EI-MS: *m/z* 274 (M⁺).

2,7-dibromo-9,9-bis(6-dioctylphosphine oxide hexyl)-9H-fluorene (4)

To a suspension of NaH (8 mmol) in anhydrous THF (10 mL) was added a solution of **2** (1.32 g, 4.8 mmol) in THF (40 mL) dropwise. The mixture was refluxed for 1 h, and then was transferred to a solution of 2,7-dibromo-9,9-bis(6-bromohexyl)-9H-fluorene (1.3 g, 2 mmol) in anhydrous THF dropwise. The mixture was refluxed for 6 h. After removal of the solvents under reduced pressure, the residue was purified by column chromatography using petroleum ether-EtOAc-CH₃OH mixture (5:1:0 to 0:100:5) as eluents to give **4** as a light yellow oil (1.49 g, 72%). ¹H NMR (300 MHz, CDCl₃, ppm): δ = 7.42–7.54 (m, 6H), 1.89–1.94 (t, *J* = 8.1 Hz, 4H), 1.88–1.63 (m, 72H), 0.85–0.90 (t, *J* = 6.6 Hz, 12H), 0.56 (m, 4H). ¹³C NMR (75 MHz, CDCl₃, ppm): δ = 151.6, 138.5, 129.8, 125.5, 121.0, 120.8, 55.0, 39.5, 31.3, 30.7, 30.5, 30.3, 30.1, 28.8, 28.6, 27.8, 26.9, 22.9, 22.1, 21.1, 13.6. ESI MS: *m/z* = 1035.5 [M + H]⁺.

2,7-Bis(4,4,5,5-tetramethyl-1,3,2-dioxaborolan-2-yl)-9,9-dihexylfluorene (6)

A mixture of 2,7-dibromo-9,9-dihexylfluorene (15 g, 30.5 mmol), KOAc (18 g, 183 mmol), bis(pinacolato)diborane (16.4 g, 64 mmol), and Pd(dppf)Cl₂ (1.8 g, 0.22 mmol) in 1,4-dioxane (150 mL) was stirred for 12 h at 80 °C. After being cooled to room temperature, water and chloroform were added into the mixture, the organic layer was washed with brine, and then dried over anhydrous Na₂SO₄. After removal of the solvent under reduced pressure, the residue was purified over silica gel column chromatography with petroleum as the eluent to give **6** as a white solid (13.4 g, 75%). ¹H NMR (300 MHz, CDCl₃, ppm): δ = 7.70–7.81 (m, 6H), 1.39 (s, 24H), 1.01–1.11 (m, 12H), 0.72–0.76 (t, *J* = 6.9 Hz, 6H).

PFH-PO-40-1 (P1)

Compounds **4** (40 mg, 0.049 mmol), **5** (468 mg, 0.951 mmol), **6** (586 mg, 1 mmol), Pd(PPh₃)₄ (24 mg, 0.02 mmol), 2–3 drops of aliquat 336, and 1.66 g of K₂CO₃ was added into a two-neck flask and degassed by N₂, then degassed toluene (11 mL) and deionized water (6 mL) were injected by syringe. The mixture was stirred under nitrogen purge at 95 °C for 48 h. After cooling to room temperature, water and chloroform were added, the separated organic layer was washed with brine and water, and then dried over anhydrous Na₂SO₄. After removal of the solvent under reduced pressure, the residue was added to stirred methanol to give a

precipitate. The precipitate was dissolved in chloroform and reprecipitated from methanol. The resulting precipitate was placed in a Soxhlet apparatus and extracted with refluxed acetone for 48 h to remove small molecules and catalyst residue, and then was dried at 60 °C in a vacuum oven to give **P1** as a light yellow solid (675 mg, 86%). ¹H NMR (300 MHz, CDCl₃, ppm): δ=7.68–7.86 (m, 8H), 2.11–2.12 (m, 4H), 0.88–1.26 (m, 17H), 0.77–0.87 (m, 10H). ¹³C NMR (50 MHz, CDCl₃, ppm): δ=152.0, 140.8, 140.2, 132.3, 129.0, 128.8, 128.6, 127.4, 126.4, 121.8, 120.2, 55.6, 40.6, 31.7, 29.9, 29.2, 24.1, 22.8, 21.8, 14.2. FT-IR (KBr): 2926, 2853, 1636, 1457, 1250, 1117, 885, 813 cm⁻¹.

PFH-PO-20-1 (**P2**)

This polymer was prepared following the similar procedures used to prepare polymer **P1** as a light yellow solid (674 mg, 83%). ¹H NMR (300 MHz, CDCl₃, ppm): δ=7.68–7.86 (m, 8H), 1.76–2.12 (m, 5H), 1.15–1.26 (m, 18H), 0.80–0.88 (m, 10H). ¹³C NMR (50 MHz, CDCl₃, ppm): δ=152.0, 140.8, 140.2, 132.5, 132.3, 129.0, 128.8, 128.6, 127.4, 126.4, 121.8, 120.2, 55.6, 40.6, 32.0, 31.6, 31.0, 29.9, 29.2, 27.2, 25.9, 24.1, 22.8, 21.6, 14.2. FT-IR (KBr): 2925, 2851, 1633, 1457, 1249, 884, 813 cm⁻¹.

PFH-PO-10-1 (**P3**)

This polymer was prepared following the similar procedures used to prepare polymer **P1** as a light yellow solid (733 mg, 85%). ¹H NMR (300 MHz, CDCl₃, ppm): δ=7.68–7.86 (m, 8H), 2.11–2.13 (m, 4H), 1.26–1.52 (m, 20H), 0.77–0.88 (m, 11H). ¹³C NMR (50 MHz, CDCl₃, ppm): δ=152.0, 151.7, 140.8, 140.2, 132.5, 132.3, 129.0, 128.8, 128.5, 127.4, 126.4, 121.8, 120.2, 55.5, 40.6, 32.0, 31.7, 31.4, 31.1, 29.9, 29.6, 29.2, 27.8, 26.5, 24.1, 22.8, 21.7, 14.2. FT-IR (KBr): 2924, 2851, 1637, 1457, 1249, 998, 884, 813 cm⁻¹.

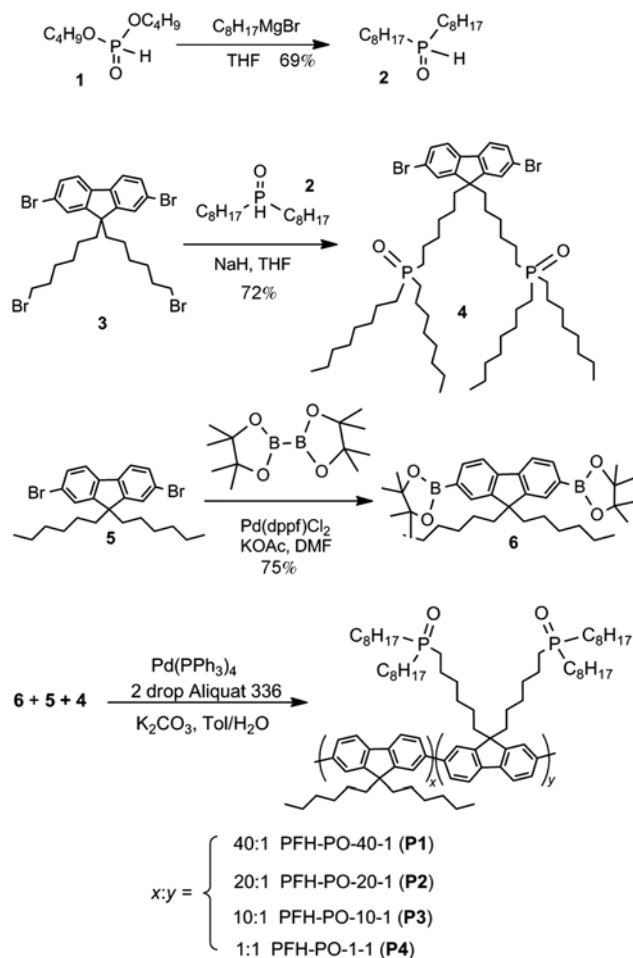
PFH-PO-1-1 (**P4**)

This polymer was prepared following the similar procedures used to prepare polymer **P1** as a light yellow solid (778 mg, 64%). ¹H NMR (300 MHz, CDCl₃, ppm): δ 7.67–7.87 (m, 16H), 2.13 (m, 8H), 0.78–1.56 (m, 128H). ¹³C NMR (50 MHz, CDCl₃, ppm): δ 152.0, 151.6, 140.7, 140.5, 140.2, 126.4, 121.5, 120.2, 55.6, 55.4, 40.5, 31.9, 31.6, 31.4, 31.1, 29.8, 29.6, 29.2, 26.9, 24.0, 22.8, 21.8, 14.2. FT-IR (KBr): 2925, 2852, 1636, 1452, 1147, 813 cm⁻¹.

3 Results and discussion

3.1 Synthesis of polymers **P1**–**P4** and characterization

Scheme 1 illustrates a synthetic approach to monomers **4** and **6**. The reaction of di-*n*-butylphosphite (**1**) with C₈H₁₇MgBr afforded dioctylphosphine oxide (**2**) with a 69% yield, which was followed by the S_N2 reaction with 2,7-dibromo-9,9-bis(6-bromohexyl)-9*H*-fluorene (**3**) to give 2,7-dibromo-9,9-



Scheme 1 The synthetic route to these polymers.

bis(6-dioctylphosphine oxide hexyl)-9*H*-fluorene (**4**) with a 72% yield. 2,7-Dibromo-9,9-dihexylfluorene (**5**) reacted with 4,4,4',5,5,5'-octamethyl-2,2'-bi(1,3,2-dioxaborolane) to afford 2,7-bis(4,4,5,5-tetramethyl-1,3,2-dioxaborolan-2-yl)-9,9-dihexylfluorene (**6**) with a 75% yield.

Monomers **4** and **5** with different ratios were polymerized with monomer **6** via a palladium-mediated Suzuki cross-coupling reaction to afford four corresponding phosphonic-functionalized polymers **P1**, **P2**, **P3**, and **P4**, respectively, as shown in Scheme 1. The crude polymers were washed with methanol, water, and methanol again, successively, and were placed in a Soxhlet apparatus and extracted with refluxed acetone for 48 h, and then were dried at 60 °C in a vacuum oven. These polymers were readily soluble in common organic solvents, such as THF, CHCl₃, and toluene. Therefore, their basic chemical structures were clearly determined by ¹H and ¹³C NMR, and FT-IR. The FT-IR feature with characteristics of 1633–1637 cm⁻¹ was proved the existence of P=O groups in these polymers. The molecular weights of these polymers were determined by gel permeation chromatography (GPC) with THF as the eluent, calibrated against polystyrene standards. As shown in Table 1,

Table 1 Molecular weight and absorption and photoluminescence properties of **P1–P4** in dilute solutions (1.0×10^{-6} M) and in thin films at room temperature

| Polymer | M_n | M_w | PDI | UV-vis λ_{\max}^a (nm) | PL λ_{\max}^a (nm) | UV-vis λ_{\max}^b (nm) | PL λ_{\max}^b (nm) |
|-----------|-------|-------|-----|--------------------------------|----------------------------|--------------------------------|----------------------------|
| P1 | 12215 | 24166 | 1.9 | 383 | 418, 441 | 379 | 445 |
| P2 | 12224 | 23614 | 1.9 | 389 | 419, 441 | 381 | 444 |
| P3 | 10134 | 18364 | 1.8 | 390 | 418, 441 | 381 | 449 |
| P4 | 3960 | 5148 | 1.3 | 387 | 419, 440 | 389 | 450 |

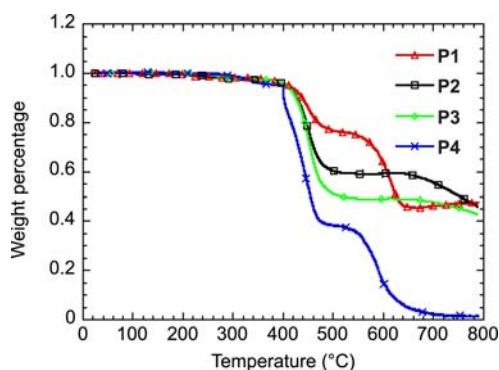
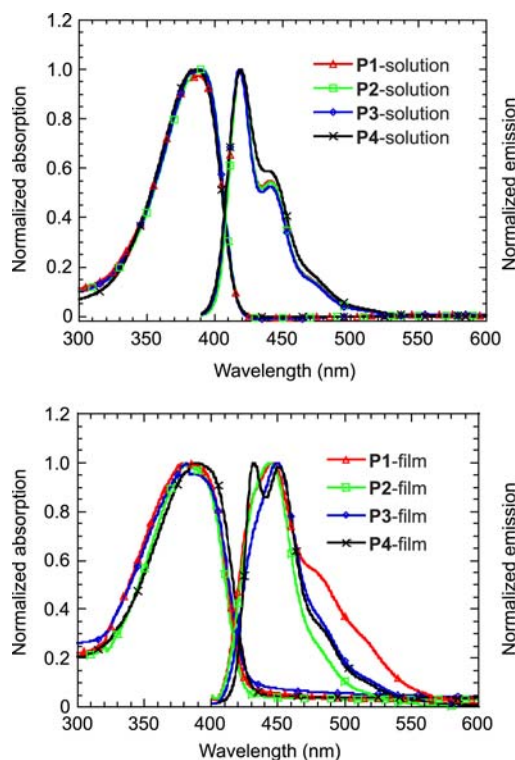
a) In dilute THF solutions (1.0×10^{-6} M) at room temperature. b) In thin films.

the GPC analysis indicated that the number-average molecular weight (M_n) and polydispersity index (PDI) of these polymers were in the ranges from 3960 to 24166 and from 1.3 to 1.9, respectively.

The thermal stability of polymers was investigated by thermogravimetric analysis (TGA) under nitrogen atmosphere. As shown in Figure 1, the onset degradation temperature of **P1–P4** was about 300 °C under nitrogen atmosphere. Differential scanning calorimetry (DSC) was used to determine the thermally induced phase transition behaviors of **P1–P4** under nitrogen atmosphere at a heating rate of $10 \text{ }^\circ\text{C min}^{-1}$. However, unlike typical poly(9,9-dialkylfluorene)s (**PAFs**), DSC measurement of **P1–P3** did not show any phase transition in the temperature range from 0 to 300 °C, except that **P4** showed a low T_g at about 80 °C which might be due to low molecular weight or too many alkyl chains in the polymer.

3.2 Photophysical and electrochemical properties

Figure 2(a) shows normalized UV-vis absorption and photoluminescence (PL) spectra of polymers **P1**, **P2**, **P3**, and **P4** in dilute THF solutions at a concentration of 1×10^{-6} M based on the polymer repeat unit. These polymers showed the same absorption and emission features in dilute solution as homopolymer poly(9,9-dihexylfluorene) [9]. The photophysical properties of these polymers in dilute solutions are summarized in Table 1. As illustrated in Figure 2(a), polymers **P1–P4** exhibited similar absorption maximum λ_{\max} (383 nm for **P1**, 390 nm for **P2**, 389 nm for **P3**, 387 nm for **P4**), which was not affected by the ratio of P=O groups in

**Figure 1** Thermal gravimetric analysis of **P1–P4** in nitrogen atmosphere.**Figure 2** Normalized UV-vis absorption and PL spectra of **P1–P4**, in dilute solutions (1×10^{-6} M based on the polymer repeat unit) and in thin film. UV-vis absorption spectra and PL spectra in dilute solutions (top); (b): UV-vis absorption spectra and PL spectra in thin film (down).

these polymers. The PL spectra of **P1**, **P2**, **P3**, and **P4** in dilute THF solutions, excited at the absorption maximum wavelength, showed almost identical PL behaviors. Their emission features peaked at about 418 nm with a clear vibronic shoulder at 441 nm, which indicated that these polymers exhibited well-extended chain conformation due to their good solubility in THF [10]. These five polymers also showed very small Stokes shifts (about 30 nm) between the 0–0 transition of absorption and emission, indicating a little structural reorganization in the excited state [11].

We also measured their absorption and emission properties in thin solid films (as shown in Figure 2(b)). The photophysical properties of these polymers in thin films are summarized in Table 2 as well. The absorption features of polymers **P1–P4** in thin films were almost identical to those in dilute solutions. Their emission features showed single broad peaks at about 445 nm except **P4**, compared with

Table 2 Electrochemical properties of **P1–P4** in thin film

| Polymer | E_{ox} (V) | E_{red} (V) | HOMO (eV) | LUMO (eV) | E_{gap} (eV) |
|-----------|---------------------|----------------------|-----------|-----------|-----------------------|
| P1 | 1.17 | -1.85 | -5.57 | -2.55 | 3.02 |
| P2 | 1.19 | -1.90 | -5.59 | -2.50 | 3.09 |
| P3 | 1.20 | -1.92 | -5.60 | -2.48 | 3.12 |
| P4 | 1.30 | -2.00 | -5.70 | -2.40 | 3.30 |

those in dilute solutions, which might be caused by some degree of aggregation in the excited states of the polymers' main chains.

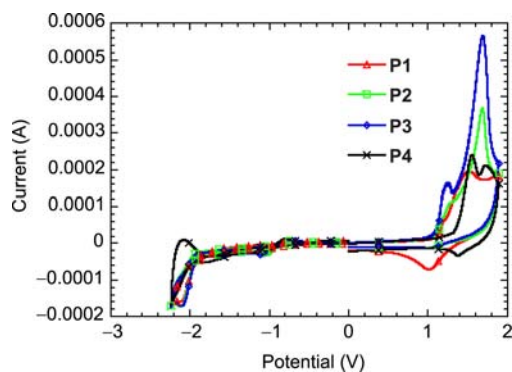
The electrochemical behavior of these polymers, as shown in Figure 3, was investigated by cyclic voltammetry (CV). The CV was performed in a solution of $n\text{-Bu}_4\text{NPF}_6$ (0.1 M) in acetonitrile at a scan rate of 100 mV/s at room temperature under the protection of nitrogen. A carbon electrode coated with a thin polymer film was used as the working electrode. A platinum wire was used as the counter electrode, and all potentials were recorded versus Ag/AgCl (saturated) as a reference electrode. The oxidation and reduction peaks appeared at 1.2 to 1.5 V and -2.1 to -2.2 V, respectively, which were attributed to the oxidation and reduction potentials for the polymers' main chains. The HOMO and LUMO levels calculated according to an empirical formula [12],

$$E_{\text{HOMO}} = -e(E_{\text{ox}} + 4.4)(\text{eV}), \text{ and } E_{\text{LUMO}} = -e(E_{\text{red}} + 4.4)(\text{eV}),$$

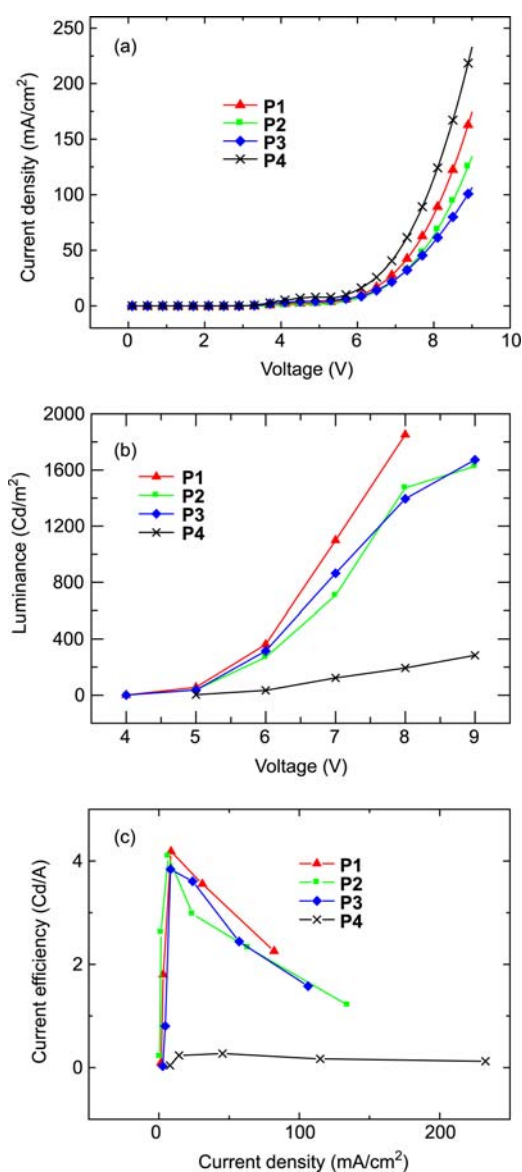
Table 2 illustrates the electrochemical properties of **P1–P4**. From the electrochemical data, it was estimated that the band gap of these functionalized polymers was around 3.02–3.30 eV for **P1–P4**.

3.3 Electroluminescence properties

The electroluminescence (EL) properties of these polymers were recorded on an organic light-emitting diode (OLED) device configuration of ITO/PEDOT:PSS/polymer/Alq₃/LiF/Al. Alq₃ worked as an electron-transport-layer in the

**Figure 3** Cyclic voltammograms of **P1–P4** in thin film coated on carbon electrodes in 0.1 mol/L Bu_4NPF_6 , CH_3CN solution.

devices. The ITO-coated glass substrate (200 nm, $20\Omega/\square$) was cleaned with the ultrasonic wave in acetone, ethanol and purified water. PEDOT:PSS was coated by spin casting and dried at 150 °C for 30 min. These polymers were coated by spin casting from a chloroform solution with a concentration of 5 mg/mL. Then Alq₃ (10 nm), LiF (1.5 nm), and Al

**Figure 4** The characteristics of the OLED devices. Current density-Voltage characteristics (a), luminance-voltage characteristics (b), current efficiency-current density characteristics (c).

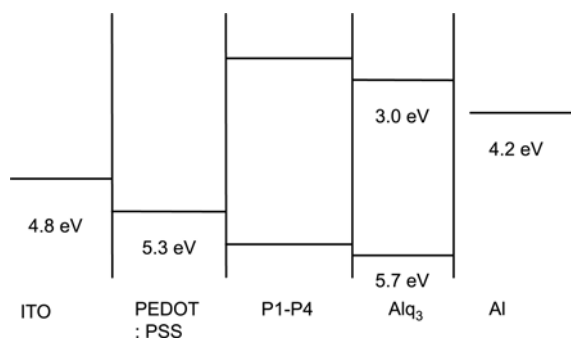


Figure 5 Energy level of the OLED devices.

Table 3 Electrochemical properties of **P1–P4** in thin film

| Polymer | E_{ox} (V) | E_{red} (V) | HOMO (eV) | LUMO (eV) | E_{gap} (eV) |
|-----------|------------------------|-------------------------|--------------|--------------|--------------------------|
| P1 | 1.17 | -1.85 | -5.57 | -2.55 | 3.02 |
| P2 | 1.19 | -1.90 | -5.59 | -2.50 | 3.09 |
| P3 | 1.20 | -1.92 | -5.60 | -2.48 | 3.12 |
| P4 | 1.30 | -2.00 | -5.70 | -2.40 | 3.30 |

(100 nm) as cathode were thermally evaporated in a vacuum chamber under a pressure of $\sim 8 \times 10^{-7}$ Torr. The current density-voltage characteristics of the OLEDs were determined with a Keithley source meter (model 2420). The luminance values were measured with a Minolta luminance meter (model LS-110).

Figure 4 shows the characterizations of the OLED devices. The best device result (Current efficiency was 4.2 Cd/A at 6V) was got from Polymer **P1**. Since the device performance of OLED was influenced by the energy barriers for charge carriers, the OLED devices with polymer **P1** showed the best performance because holes and electrons had the smallest energy barrier in the devices (as shown in Figure 5) according to the electrochemical properties (as shown in Table 3).

4 Conclusions

In conclusion, we synthesized four new polyfluorene derivatives **P1**, **P2**, **P3** and **P4** via a Suzuki polymerization. These polymers are the first examples of PF copolymer derivatives with phosphine oxide groups in the side chains. These polymers possess good thermal stability, large band gap, and good film-forming properties. Their emission features showed single broad peaks at about 445 nm except **P4**, compared with those in dilute solutions, which might be caused by some degree of aggregation in the excited states of the polymers' main chains. The electroluminescence (EL) properties of these polymers were recorded on an organic light-emitting diode (OLED) device configuration of ITO/PEDOT:PSS/Polymer/Alq₃/LiF/Al. The best device

result (Current efficiency was 4.2 Cd/A at 6 V) was got from Polymer **P1**, which might be due to that the hole and electron in this device had the smallest energy barrier. More detailed work on optimizing devices and device performance is in progress.

This work was supported by the National Basic Research Program of China (2006CB921602 and 2009CB623601) and National Natural Science Foundation of China, and Hewlett Packard Company.

- (a) Braun D, Heeger AJ. Visible light emission from semiconducting polymer diodes. *Appl Phys Lett*, 1991, 58: 1982–1986; (b) Burns PL, Holmes AB, Kraft A, Bradley DDC, Brown AR, Friend RH, Gymer RW. Chemical tuning of electroluminescent copolymers to improve emission efficiencies and allow patterning. *Nature*, 1992, 356: 47–49; (c) Pei Q, Yu G, Zhang C, Yang Y, Heeger AJ. Polymer light-emitting electrochemical cells. *Science*, 1995, 269: 1086–1088; (d) Müller CD, Falcou A, Reckefuss N, Rojahn M, Wiederhorn V, Rudati P, Frohne H, Nuyken O, Becker H, Meerholz K. Multi-colour organic light-emitting displays by solution processing. *Nature*, 2003, 421: 829–833
- (a) Lovinger AJ, Rothberg LJ. Status of and prospects for organic electroluminescence. *J Mater Res*, 1996, 11: 3174–3187; (b) Bao Z, Lovinger AJ, Brown J. New air-stable n-channel organic thin film transistors. *J Am Chem Soc*, 1998, 120: 207–208; (c) Bao Z, Dodabalapur A, Lovinger AJ. Soluble and processable regioregular poly(3-hexylthiophene) for thin film field-effect transistor applications with high mobility. *Appl Phys Lett*, 1996, 69: 4108–4110; (d) Sirringhaus H, Tessler N, Friend RH. Integrated optoelectronic devices based on conjugated polymers. *Science*, 1998, 280: 1741–1744; (e) Babel A, Jenekhe SA. Electron transport in thin-film transistor from an n-type conjugated polymer. *Adv Mater*, 2002, 14: 371–374
- (a) Tang CW. Two-layer organic photovoltaic cell. *Appl Phys Lett*, 1986, 48: 183–185; (b) Wohrle D, Meissner D. Organic solar cell. *Adv Mater*, 1991, 3: 129–138; (c) Yu G, Heeger AJ. Charge separation and photovoltaic conversion in polymer composites with internal donor/acceptor heterojunctions. *J Appl Phys*, 1995, 78: 4510–4515; (d) Arias AC, MacKenzie JD, Stevenson R, Halls JJM, Inbasekaran M, Woo EP, Richards D, Friend RH. Photovoltaic performance and morphology of polyfluorene blends: A combined microscopic and photovoltaic investigation. *Macromolecules*, 2001, 34: 6005–6013; (e) Jenekhe SA, Yi S. Efficient photovoltaic cells from semiconducting polymer heterojunctions. *Appl Phys Lett*, 2000, 77: 2635–2637
- (a) Bernius MT, Inbasekaran M, O'Brien J, Wu WS. Progress with light-emitting polymers. *Adv Mater*, 2000, 12: 1737–1750; (b) Neher D. Polyfluorene homopolymers: Conjugated liquid-crystalline polymers for bright blue emission and polarized electroluminescence. *Macromol Rapid Commun*, 2001, 22: 1366–1385; (c) Scherf U, List EJW. Semiconducting polyfluorenes—Towards reliable structure-property relationship. *Adv Mater*, 2002, 14: 477–487; (d) Klärner G, Lee JK, Davey MH, Miller RD. Exciton migration and trapping in copolymers based on dialkylfluorenes. *Adv Mater*, 1999, 11: 115–119; (e) Yu WL, Pei J, Huang W, Heeger AJ. Spiro-functionalized polyfluorene derivatives as blue light-emitting materials. *Adv Mater*, 2000, 12: 828–831; (f) Virgili T, Lidzey DG, Bradley DDC. Efficient energy transfer from blue to red in tetraphenylporphyrin-doped poly(9,9-dioctylfluorene) light-emitting diodes. *Adv Mater*, 2000, 12: 58–62; (g) Whitehead KS, Grell M, Bradley DDC, Jandke M, Strohrig P. Highly polarized blue electroluminescence from homogeneously aligned films of poly(9,9-dioctylfluorene). *Appl Phys Lett*, 2000, 76: 2946–2948; (h) Grell M, Knoll W, Lupo D, Meisel A, Miteva T, Neher D, Nothofer HG, Scherf U, Yasuda A. Blue polarized electroluminescence from a liquid crystalline polyfluorene. *Adv Mater*, 1999, 11: 671–675
- (a) Liu B, Bazan GC. Optimization of the molecular orbital energies of conjugated polymers for optical amplification of fluorescent sen-

- sors. *J Am Chem Soc*, 2006, 128: 1188–1196; (b) Wang S, Gaylord BS, Bazan GC. Fluorescein provides a resonance gate for FRET from conjugated polymers to DNA intercalated dyes. *J Am Chem Soc*, 2004, 126: 5446–5451; (c) Liu B, Wang S, Bazan GC, Mikhailovsky A. Shape-adaptable water-soluble conjugated polymers. *J Am Chem Soc*, 2003, 125: 13306–13307; (d) Fan C, Plaxco KW, Heeger AJ. High-efficiency fluorescence quenching of conjugated polymers by proteins. *J Am Chem Soc*, 2002, 124: 5642–5643; (e) Zhou G, Cheng YX, Wang LX, Jing XB, Wang FS. Novel polyphenylenes containing phenol-substituted oxadiazole moieties as fluorescent chemosensors for fluoride ion. *Macromolecules*, 2005, 38: 2148–2153; (f) Zhou X, Yan J, Pei J. Exploiting an imidazole-functionalized polyfluorene derivative as a chemosensory material. *Macromolecules*, 2004, 37: 7078–7080; (g) Zhou G, Qian G, Ma L, Cheng YX, Xie ZY, Wang LX, Jing XB, Wang FS. Polyfluorenes with phosphonate groups in the side chains as chemosensors and electroluminescent materials. *Macromolecules*, 2005, 38: 5416–5424; (h) Qin CJ, Cheng YX, Wang LX, Jing XB, Wang FS. Phosphonate-functionalized polyfluorene as a highly water-soluble iron(III) chemosensor. *Macromolecules*, 2008, 41: 7798–7804; (i) Qin CJ, Wu XF, Gao BX, Tong H, Wang LX. Amino acid-functionalized polyfluorene as a water-soluble Hg²⁺ chemosensor with high solubility and high photoluminescence quantum yield. *Macromolecules*, 2009, 42: 5427–5433; (j) Wu X, Xu B, Tong H, Wang LX. Phosphonate-functionalized polyfluorene film sensors for sensitive detection of iron(III) in both organic and aqueous media. *Macromolecules*, 2010, 43: 8917–8921
- 6 (a) Huang F, Hou L, Wu H, Wang X, Shen H, Cao W. High-efficiency, environment-friendly electroluminescent polymers with stable high work function metal as a cathode: Green- and yellow-emitting conjugated polyfluorene polyelectrolytes and their neutral precursors. *J Am Chem Soc*, 2004, 126: 9845–9853; (b) Wu H, Huang F, Mo Y, Yang W, Wang D, Peng J. Efficient electron injection from a bilayer cathode consisting of aluminum and alcohol-/water-soluble conjugated polymers. *Adv Mater*, 2004, 16: 1826–1830; (c) Yang R, Wu H, Cao Y, Bazan GC. Control of cationic conjugated polymer performance in light emitting diodes by choice of counterion. *J Am Chem Soc*, 2006, 128: 14422–14423
- 7 Peng XG, Schlamp MC, Kadavanich AV, Alivisatos AP. Epitaxial growth of highly luminescent CdSe/CdS core/shell nanocrystals with photostability and electronic accessibility. *J Am Chem Soc*, 1997, 119: 7019–7029
- 8 Skaff H, Sill K, Emrick T. Quantum dots tailored with poly(paraphenylene vinylene). *J Am Chem Soc*, 2004, 126: 11322–11325
- 9 (a) Scherf U, List EJW. Semiconducting polyfluorenes—Towards reliable structure–property relationships. *Adv Mater*, 2002, 14: 477–487; (b) Gong X, Iyer PK, Moses D, Bazan GC, Heeger AJ, Xiao SS. Stabilized blue emission from polyfluorene-based light-emitting diodes: Elimination of fluorenone defects. *Adv Funct Mater*, 2003, 13: 325–330; (c) Gong X, Moses D, Heeger AJ. White light electrophosphorescence from polyfluorene-based light-emitting diodes: Utilization of fluorenone defects. *J Phys Chem B*, 2004, 108: 8601–8605
- 10 (a) Brooks AJ, Antonio F, Micheal RW, Tobin JM. Effects of arylene diimide thin film growth conditions on n-channel OFET performance. *Adv Funct Mater*, 2008, 18: 1329–1339; (b) Chu B, *Laser Light Scattering: Basic Principles and Practice*. 2nd ed, San Diego: Academic Press, 1991; (c) Hall J, Lehn JM, DeCian A, Fischer J. Synthesis and structure of the copper(II) complex of a chiral bis(dihydrooxazole) ligand. *Helv Chim Acta*, 1991, 74: 1–6
- 11 Yan JC, Chen X, Zhou QL, Pei J. Chiral polyfluorene derivatives: Synthesis, chiroptical properties, and investigation of the structure–property relationships. *Macromolecules*, 2007, 40: 832–839
- 12 Leeuw DM, Simenon MMJ, Brown AR, Einerhand REF. Stability of n-type doped conducting polymers and consequences for polymeric microelectronic devices. *Synth Met*, 1997, 87: 53–59